Fixed Switching Frequency Sliding Mode Control for Single Phase Unipolar Inverters

Ahmad Hani Yassen

Submitted to the
Institute of Graduate Studies and Research
in partial fulfillment of the requirements for the Degree of

Master of Science
in
Electrical and Electronic Engineering

Eastern Mediterranean University
March 2014
Gazimağusa, North Cyprus

Approval of the Institute of Graduate Studies and Research

Prof. Dr. Elvan Yılmaz
Director

I certify that this thesis satisfies the requirements as a thesis for the degree of Master of Science in Electrical and Electronic Engineering.

Prof. Dr. Aykut Hocanın
Chair, Department of Electrical and Electronic Engineering

We certify that we have read this thesis and that in our opinion it is fully adequate in scope and quality as a thesis for the degree of Master of Science in Electrical and Electronic Engineering.

Prof. Dr. Osman Kükrer
Supervisor

Examining Committee

1. Prof. Dr. Hasan Kömürcügil
2. Prof. Dr. Osman Kükrer
3. Prof. Dr. Runyi Yu

ABSTRACT

For the application of UPS inverters. The aim of the UPS is to provide the necessary loads with a sinusoidal output voltage at low harmonic distortion. The controller has to be able to handle any external disturbances may occur, and should have a fast response at low steady state error.

For that purpose; the sliding mode controller is applied to the UPS system here. Sliding mode controller has the advantage of robustness to parameter variations and disturbances, but still suffers from chattering problem when the state of the error approaches the equilibrium point.

In this thesis, the control input has been saturated in narrow boundary, aiming to reduce the chattering problem. Pulse width modulation is used to compare the smoothed control function with a reference carrier resulting a fixed switching frequency for the unipolar UPS inverter.

The output voltage of the inverter has low total harmonic distortion according to IEC62040-3 standard. The proposed controller is fast and robust as the simulations show.

Keywords: Pulse width modulation, voltage source inverter, sliding mode control.

ÖZ

Kesintisiz güç kaynakları hassas yükleri düşük harmonik bozunumlu sinüzoidal gerilim ile beslemek için kullanılır. Bir KGK'nın denetleyicisinin dış bozanetkenlerle başedebilmesi ve düşük durağan durum hatası ile hızlı tepkimeye sahip olması gerekir.

Bu amaçla KGK'ya kayan kipli denetim uygulanmıştır. Kayan kipli denetim, bozanetkenlere ve parametre değişimlerine karşı dayanıklı olmasına rağmen, durum değişkenlerinin hatası denge noktasına yaklaşırken oluşan yüksek frekanslı salınım sorununa sahiptir.

Bu tezde anahtarlamalı denetleyici çıkışı dar bir bölgede girişin doğrusal işlevidir. Bunun amacı yüksek frekanslı salınımların önüne geçmektir. Düzgün hale getirilmiş denetleyici çıkışını taşıyıcı işaret ile karşılaştırmak suretiyle darbe genişlik kiplemesi kullanılmıştır. Bu şekilde KGK evirgeçini sabit anahtarlama frekansı ile çalıştırmak mümkün olmuştur.

Evirgeç çıkış gerilimi IEC62040-3 standardına uygun olarak düşük harmonik bozunuma sahiptir. Benzetim sonuçları, önerilen denetleyicinin hızlı ve dayanıklı olduğu gözlenmiştir.

Anahtar kelimeler: Darbe genişlik kiplemesi, gerilim kaynaklı evirgeç, kayan kipli denetim.

To My Parents

ACKNOWLEDGMENTS

First, I would like to thank almighty ALLAH for finally finishing the writing of this thesis for my Master‘s degree in Electronic Engineering.

I would like to express my deepest gratitude to my supervisor Prof. Dr. Osman Kukrer for his valuable suggestions and comments; honestly, this work could not have been completed without his inspiring guidance.

I would also like to thank all department staff who gave me the support and help I needed during the writing of this thesis.

Finally, I would like to thank my parents, brothers, sister’s friends especially Hamza al Masri and Derar Zedan for their endless support and understanding during this thesis process.

TABLE OF CONTENTS

LIST OF TABLES

LIST OF FIGURES

LIST OF SYMBOLS

α	Voltage Error Coefficient
δ	Hysteresis Band Width
ϕ	Saturation Parameter
λ^{FL}	Sliding Line Slope

LIST OF ABBREVIATIONS

ASD	Adjustable Speed Drives
CSI	Current Source Inverter
GTO	Gate Turn-off Thyristor
IGBT	Insulated-Gate Bipolar Transistor
MOSFET	Metal Oxide Semiconductor Field Effect Transistor
PID	Proportional- Integral Derivative Controller
PWM	Pulse Width Modulation
RMS	Root Mean Square
STC	Self Tuning Controller
UPS	Uninterruptable Power Supply
UPWM	Uniform Pulse Width Modulation
VSC	Variable Structure Control
VSI	Voltage Source Inverter

Chapter 1

INTRODUCTION

The use of uninterruptable power supplies (UPS) has become more important because of its big contributions in the field of power quality improvement, ac motor control and renewable energy applications. The main goal required from the UPS is to provide the emergency load with the necessary power supply under all working conditions. The output voltage must be sinusoidal, with specified frequency and amplitude at low total harmonic distortion (THD), according to specified standards.

The problem of UPS inverter represents a nonlinear system, which can be controlled using the theory of sliding mode control (SMC), which is derived from the general theory of variable structure control (VSC). Although it suffers from chattering, sliding mode control has very good features including disturbance rejection and robustness to parameters variations.

There are many approaches that have been introduced in the SMC theory. A three level hysteresis function is derived from the voltage error, its rate of change and it's integral in [5]. An expression is derived to calculate the switching frequency. However, the slope of the sliding line has been derived from the fuzzy like

Input/output relationship, resulting in the rotation of the sliding line in the phase plane such that fast response is achieved.

The aim of this thesis is to investigate the possibility of using a switching function which does not involve hysteresis. It is based on the work presented in [7]. Here, the switching controller output is a linear function of the input in a narrow layer, such that the problem of chattering is reduced. The controller output is then compared with a carrier signal. The resulting PWM output waveform has a fixed switching frequency. The proposed method shows a good performance under linear, nonlinear and sudden loads. The harmonic contents are acceptable and according to the standards IEC62040-3 [7].

This thesis is organized as follows. In chapter 2, inverter types, its usage as UPS and a review for PWM techniques are presented. In chapter 3, general review for SMC theory with previous work done in this field is introduced. In chapter 4, control function derivation and design consideration is discussed and arguments are highlighted. Simulations and results are presented in chapter 5. Finally, chapter 6 derives some conclusions and future work.

Chapter 2

INVERTERS

Power electronics was invented as a result of the revolution of semiconductor devices. After the invention of the thyristor, modern power electronics were developed and many semiconductor devices such as triac, gate turn-off thyristor (GTO), bipolar power transistor (BJT), and power MOSFET, insulated gate bipolar transistor (IGBT) have gradual usage in the field of power electronics [4].

After the revolution of power electronics, the revolution of microelectronics has been started, resulting in a big progress in the field of high performance, high reliable and small size microelectronic microchip devices. In this chapter, firstly, an introduction about single phase inverters is to be presented. Then the inverter used as uninterruptable power supply (UPS) is discussed. Finally, a review of the common pulse width modulation techniques is made.

2.1 Inverters

An inverter is an electronic device which takes DC power and converts this power to AC power. The output value, frequency and phase shift are varied with respect to time by controlling the power switches of the inverter. Figure 2.1 shows the general construction of a DC/AC power converter with fixed input DC voltage and variable AC output waveform.

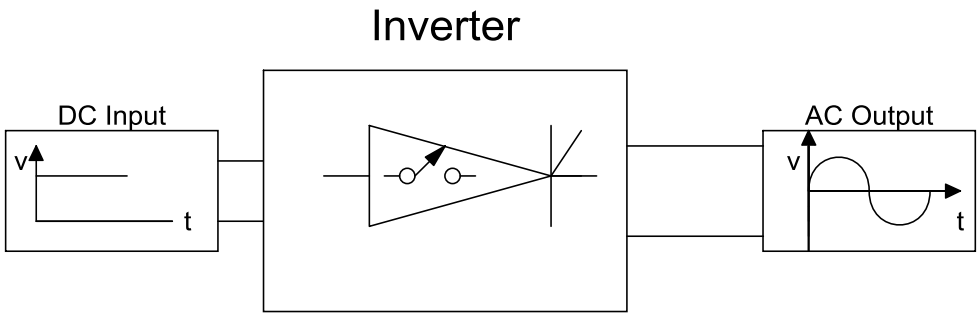

Figure 2.1: General construction of DC/AC converter.

Inverters are classified into two main types as single-phase and three-phase. If the classification is based on the input source, then we have current source inverter and voltage source inverter. When the input of the inverter is a fixed current source, then it's called current source inverter (CSI). This type is widely used in the industrial applications where high quality performance is required.

If the source of the inverter is a voltage source, then it's called a voltage source inverter (VSI). This type is used in industrial applications such as adjustable speed drives (ASD) and uninterruptable power supply (UPS) inverter [1].

Basically, the operation of any power electronics device depends on the usage of power electronics switches. These switches are made of semiconductor materials.

2.1.1 Single-Phase Half Bridge Inverter

Basically, single phase half-bridge inverter consists of two switches (semiconductor devices) S1and S2 shown in Figure 2.2. In most cases the switches are BJT, IGBT or MOSFET. Two diodes D1 and D2 are connected in parallel to the switches. The diodes are called freewheeling diodes, because they allow the negative current to pass (freewheel) through them in the opposite direction when it's needed.

If C1 and C2 which are connected in parallel with the source are exactly equal, the source is divided into two equal values by the capacitors.

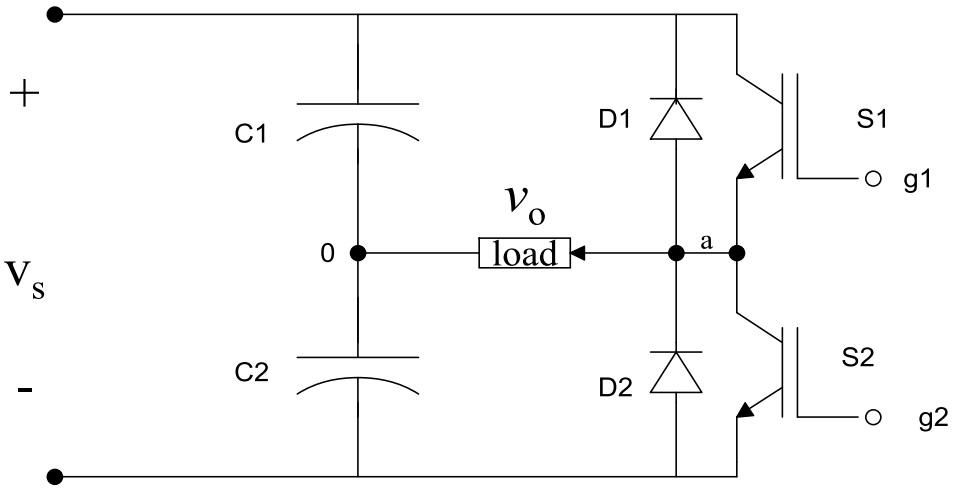

Figure 2.2: Single phase half bridge inverter [1].

Transistor S1 is controlled by control signal g1 and transistor g2 is controlled by control signal g2. Both control signals g1 and g2 can be {0,1}, if the control signal is 1, the transistor will be on and the output voltage equal to $\frac{V_s}{2}$, otherwise the transistor will be off and the output voltage equal to $-\frac{V_s}{2}$. As a result; the output voltage has two levels $\frac{V_s}{2} and -\frac{V_s}{2}$, and the switches must operate alternately to avoid short circuiting the source voltage.

2.1.2 Single Phase Full Bridge Inverter

Full-bridge inverter or H-bridge inverter consists of four semiconductor switches. Each switch has a freewheeling diode connected in parallel with it, as shown in Figure 2.3. These diodes are used as protection devices because they allow the reverse current (negative current) to pass through them.

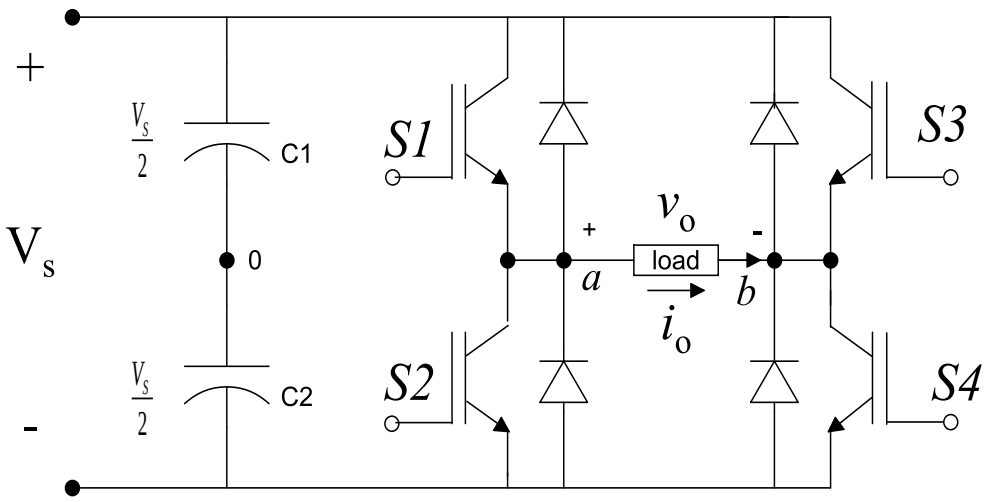

Figure 2.3: Single Phase full Bridge Inverter [2].

When the switch devices S1 and S4 are on, and S2 and S3 are off then V_{a0} and V_{b0} are equal to $\frac{V_S}{2}, -\frac{V_S}{2}$ respectively, and the output will be V_s. Similarly, if S3 and S2 are on and S1and S4 are off, then V_{a0} and V_{b0} are equal to $-\frac{V_S}{2}, \frac{V_S}{2}$ respectively, and the output will be -V_s. Table 1.1 shows the main possible switching states of the inverter.

Table 2.1: Switching states for single-phase H-bridge inverter [3].

S_1	S_2	S_3	S_4	V_{a0}	V_{b0}	V_{ab}
ON	OFF	OFF	ON	$\frac{V_S}{2}$	$-\frac{V_S}{2}$	V_S
OFF	ON	ON	OFF	$-\frac{V_S}{2}$	$\frac{V_S}{2}$	$-V_S$
ON	OFF	ON	OFF	$\frac{V_S}{2}$	$\frac{V_S}{2}$	0
OFF	ON	OFF	ON	$-\frac{V_S}{2}$	$-\frac{V_S}{2}$	0

If the switching sequence in Table 2.1 is applied to the H-bridge inverter, the output voltage signal waveforms will be as shown in Figure 2.4.

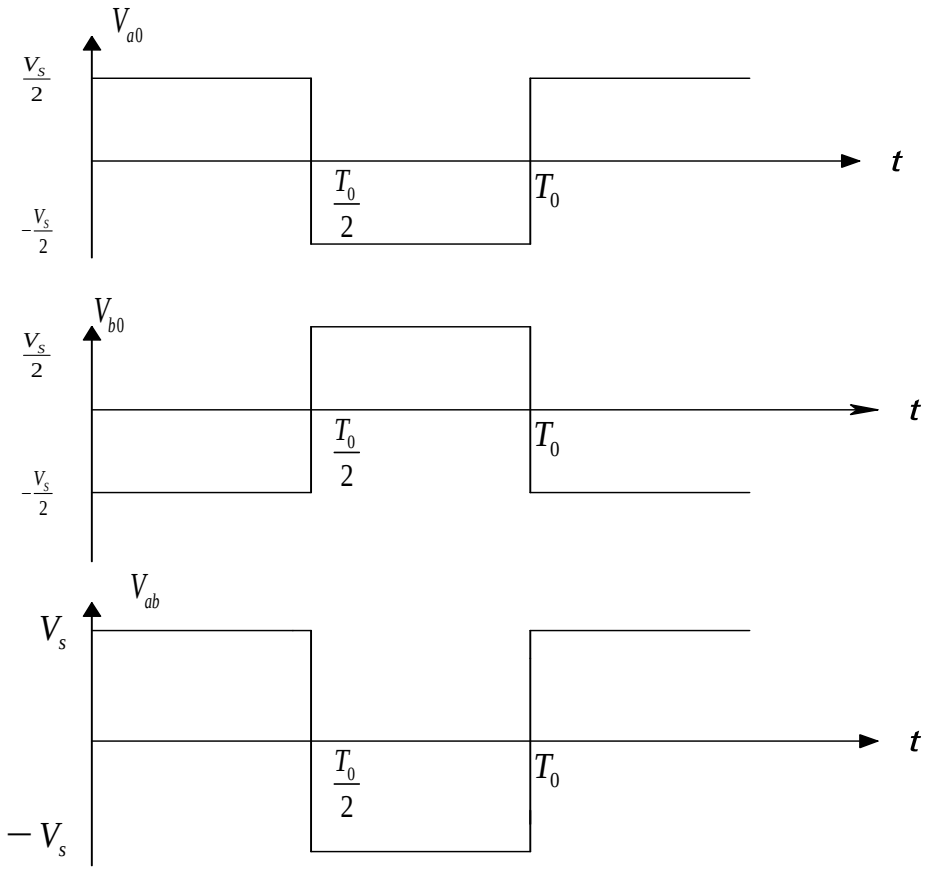

Figure 2.4: Output voltage waveforms for square wave operation [2].

2.2 Inverter Used as a UPS Inverter

UPS inverter is used to provide emergency AC power supply to the load during system power failure. In case of power supply fluctuations or failure, inverters should be able to supply the loads till the standby generators are started, or till the organized shut down is done. Figure 2.5 and Figure 2.6 show the main construction of two main types of UPS inverters.

2.2.1 Online Backup UPS System

This type is continuously connected to the online network as shown in Figure 2.5. In this case the inverter supplies the critical load with steady, clean AC power (pure AC power) even when the main power supply is available. This type is recharged always from the main power supply source.

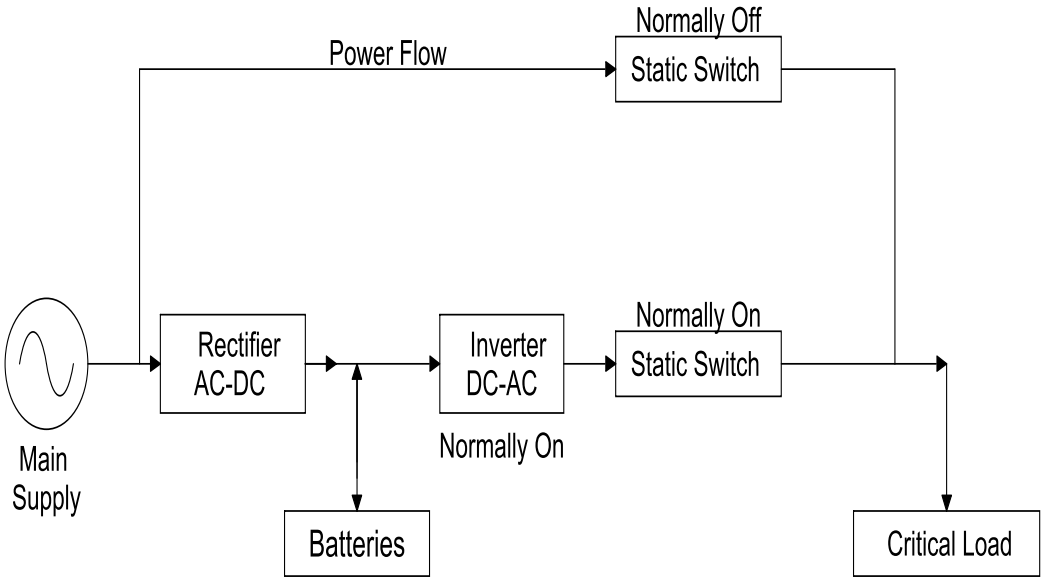

Figure 2.5: Online backup UPS system.

2.2.2 Standby UPS System

This type is also called offline backup UPS system and is shown in Figure 2.6. In this type, the main power supply is normally connected to the load and the UPS is connected to the critical load only when there is power fluctuation or if there is power failure. The batteries are recharged from the main supply only when they are not in service.

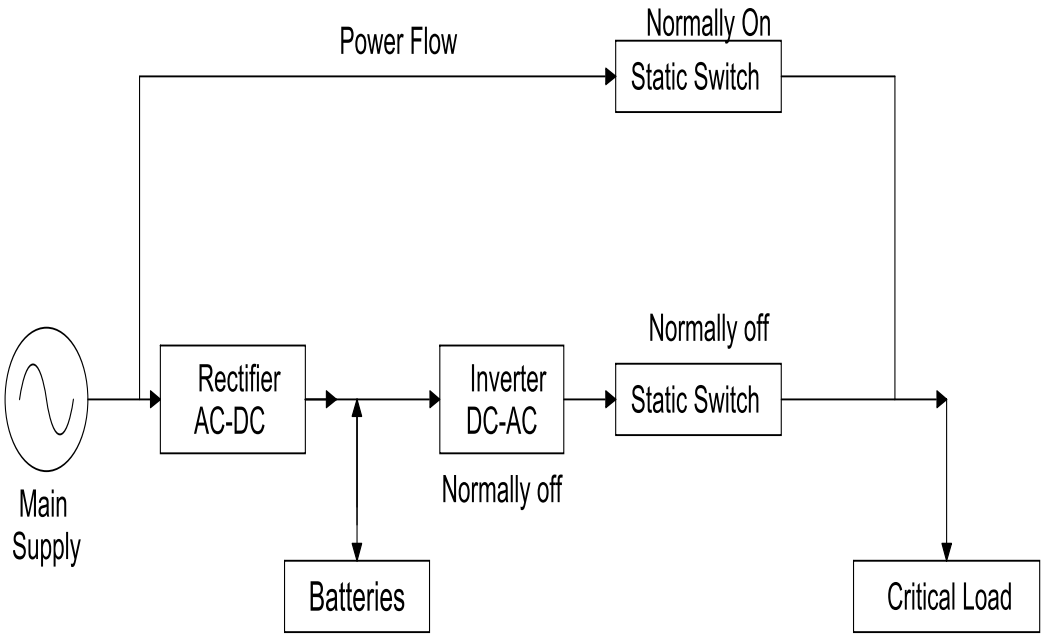

Figure 2.6: Standby UPS system.

A UPS is designed to work under critical conditions to supply the emergency loads such as hospitals, computer labs, emergency lights and alarm systems. The output of the UPS is pure sinusoidal at low harmonic distortion with fast transient response. All these factors together give an indication about the performance of the UPS [12].

2.3 PWM Techniques

There are many techniques to control inverters such that some or all of the above requirements are achieved. PWM is the most famous and simple way of controlling the inverter. And here we introduce and define some of the PWM techniques.

2.3.1 Single Pulse Width Modulation

In single PWM control there is one pulse in each half cycle. In this method the width of each pulse is changeable to control the output voltage. Figure 2.7 shows the gate signal, generation procedure for this method and the output of single phase full bridge inverter.

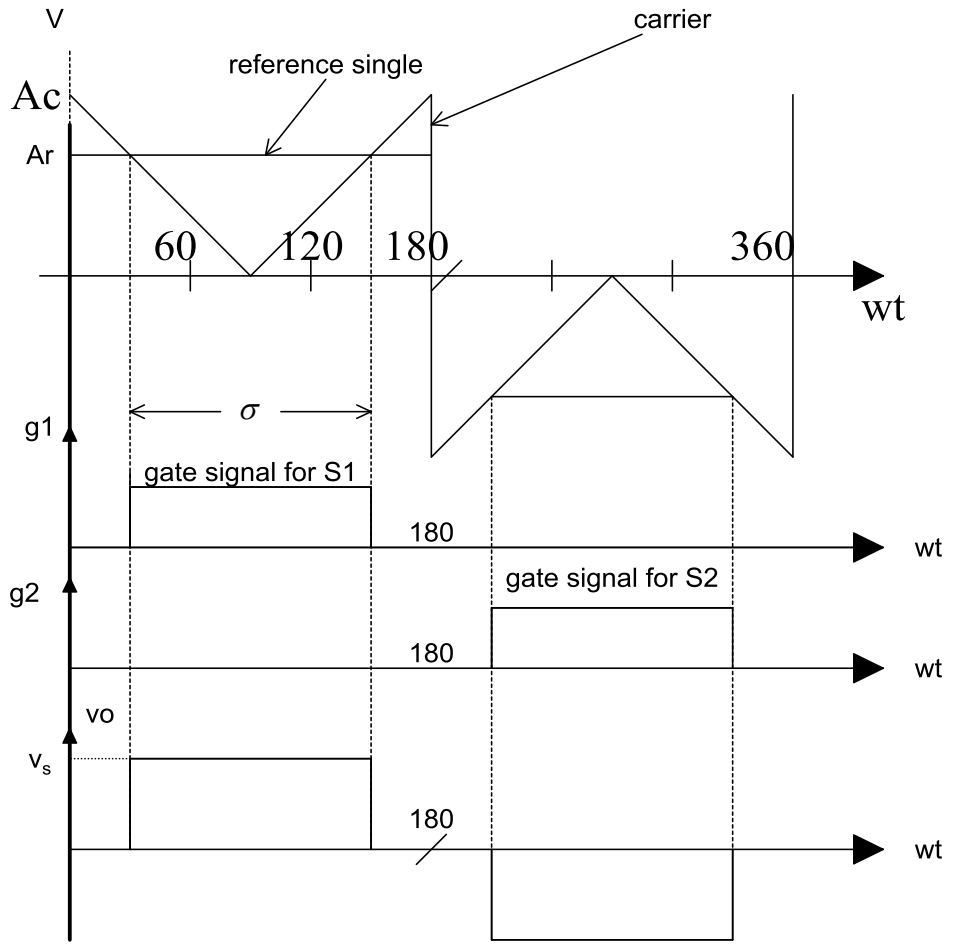

Figure 2.7: Single PWM gate signal and output waveforms of full H-inverter [3].

The pulse signal is generated by comparing the amplitude of the triangular carrier wave (A_c) with the amplitude of rectangular signal (A_r). The frequency of the output voltage is determined by the frequency of the reference voltage. The instantaneous output voltage equals $v_o = V_s(g_1 - g_2)$. The ratio between A_c and A_r is defined as the modulation index $m_a = \frac{A_C}{A_r}$. The root-mean-square (rms) output voltage is given as $V_{o,rms} = V_s\sqrt{\frac{\sigma}{\pi}}$ where σ is the is the on-time period.

2.3.2 Multiple Pulse Width Modulation (MPWM)

This type is called uniform pulse width modulation (UPWM). In general, the MPWM generates more than one pulse per half cycle as shown in Figure 2.8. The pulses (gating signals) are generated by comparing the amplitude of the triangular carrier wave A_c with the amplitude of a rectangular signal. The frequency of the output voltage f_o is determined by the frequency of the reference voltage and the frequency of the carrier f_c. The number of pulses per half cycle are given by $p = \frac{f_c}{2f_o}$

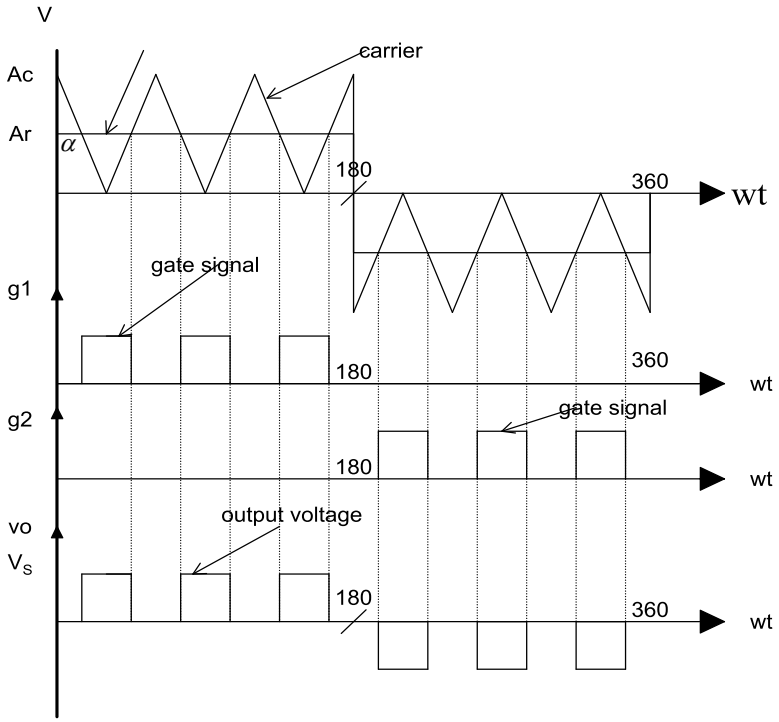

Figure 2.8: MPWM gating signals and output voltage waveform [3].

2.3.3 Sinusoidal Pulse Width Modulation (SPWM)

In the MPWM the widths of the pulses are the same but in SPWM each pulse has different width because this technique has sinusoidal reference signal. The pulses are generated by comparing the triangular signal (carrier wave) with sinusoidal signals as shown in Figure 2.9. The sinusoidal signal is used as reference and the frequency of the this signal f_r determines the output frequency f_o, and the carrier frequency determines the number of pulses in each half cycle [12].

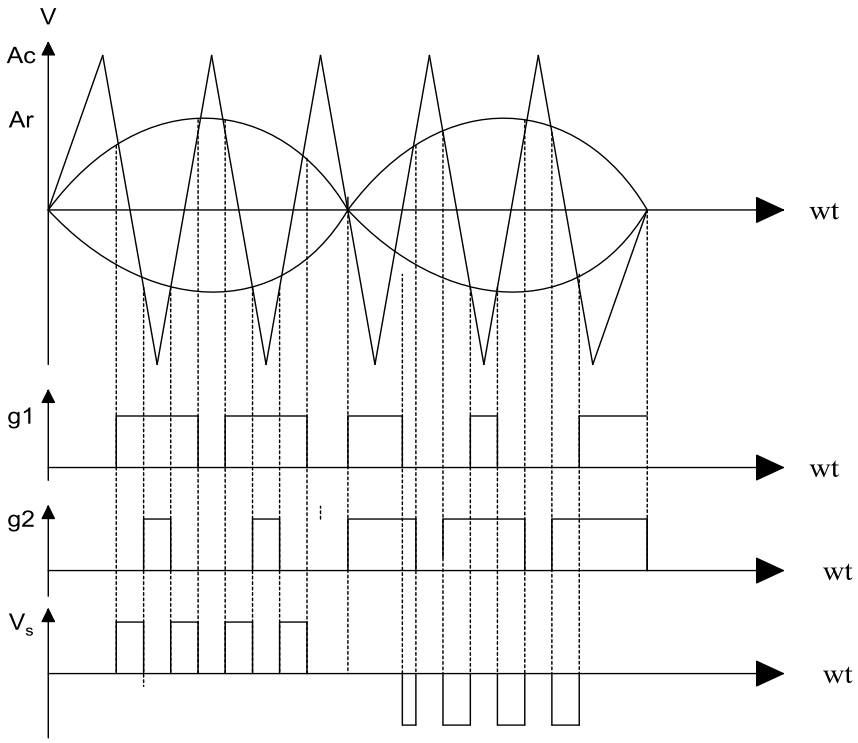

Figure 2.9: SPWM gating signals and inverter output voltage waveforms [12].

Chapter 3

SMC THEORY

Variable structure control theory (VSC) was first established in the Soviet Union in 1950's. The main design issue in SMC theory is to design proper switching function modes which guarantee system stability. The theory of sliding mode was derived from VSC theory, which is applied to nonlinear and discontinuous control systems. This method describes the nonlinear system behavior and dynamics.

The theory proposes a high switching frequency input to be applied to the system such that stability is guaranteed. The switching input varies from one state to another at high speed to achieve the desired stability. The plant model order will be reduced to a lower order to guarantee the stability in finite time, in addition to the robustness of the system. Robustness is one of the main features of SMC theory and presented as "disturbance rejection''.

While SMC has very good properties, it still suffers from the chattering problem which is defined to be the zigzag behavior that occurs on the sliding line during the convergence of the state toward the equilibrium point. Here a control strategy to reduce chattering is presented.

3.1 Reaching Condition

Designing the reaching mode is a very critical condition to ensure that all the states will reach the sliding line, and will ensure the designed dynamic during the transient period, when the disturbances are applied to the system. There are many conditions to ensure the reaching condition presented in [11]. So the reaching condition is to be applied to the system such that all the states will move toward sliding surface.

Here we are we are going to present some of the reaching conditions:

1. The direct switching function approach

   Normally used for single input VSC systems. It's not applicable for multiple input VSC systems and remains difficult to be implemented. The condition is given by

$$s(x)s^{\bullet}(x) < 0 \tag{3. 1}$$

   The condition states that the sliding line may or may not belong to the sliding manifold. But, still applicable to be a reaching condition.

2. The Lyapunov function approach

   This condition ensures that all the state space will eventually become sliding and will eventually reach the sliding line. A global reaching could be established by the condition

$$s^T s < 0 \ when \ s \neq 0 \tag{3.2}$$

   And finite reaching time could be established by

$$V^{\bullet}(x,t) < -\varepsilon \qquad \text{when } s \neq 0 \tag{3.3}$$

where $V^{\bullet}(x,t) = s^T s$ and ε is positive.

3. The reaching law approach

   The reaching law is given by

$$s^{\bullet} = -Q\,\mathrm{sgn}(s) - Kf(s) \tag{3.4}$$

   where Q and K are diagonal matrices with positive elements. The choice of Q and K could be established by one of the following approaches for the reaching law.

   a) The constant rate

$$s^{\bullet} = -Q\,\mathrm{sgn}(s) \tag{3.5}$$

   b) The proportional rate

$$s^{\bullet} = -Q\,\mathrm{sgn}(s) - Ks \tag{3.6}$$

   c) The power rate

$$\dot{s}_i = -K_i \left|s_i\right|^{\alpha} \mathrm{sgn}(s_i) \quad 0 < \alpha < 1,\ i = 1 \text{ to } m \tag{3.7}$$

3.2 Reaching Mode and Sliding Mode

Reaching mode is defined to be the trajectory path where the states go from any point on the phase plane till they reach the sliding line. The sliding line is defined to be the line where the states slide on it till it reaches the equilibrium point. Figure 3.1 describes all the previous definitions.

The condition of the sliding mode to exist is given by

$$\lim_{s \to -0} s^{\bullet} > 0 \ \text{ And } \ \lim_{s \to +0} s^{\bullet} < 0 \tag{3.8}$$

Both conditions are to be satisfied together.

3.3 The Continuation Approach of Sliding Mode

In the sliding mode theory, a discontinuous control input is to be used in the feedback control at high frequency such that controllability is achieved. The ideal control is given by

$$u = \begin{cases} u^{+}(x,t)\ ,\ s(x)>0 \\ u^{-}(x,t)\ ,\ s(x)<0 \end{cases} \tag{3.9}$$

Because it's impossible to switch from $u^{+}(x,t)\ to\ u^{-}(x,t)$ in zero time. It's impossible to implement such a switch in practice. To reduce chattering it's common to replace the ideal switch by a saturation continuous approximation [11]. There are several approaches to overcome the chattering problem as presented in [11].

a) The ideal relay control

The ideal relay is shown in Figure 3.1 which is described by

$$u(s) = \begin{cases} +1 & s(x) > 0 \\ -1 & s(x) < 0 \end{cases} \tag{3.10}$$

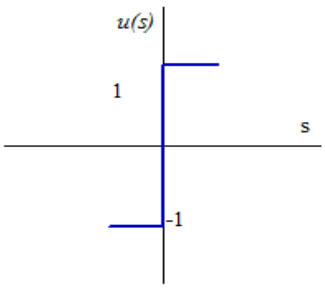

Figure 3.1: Ideal control relay.

The switching changes instantly between {+1 and -1} at s=0. This switch cannot eliminate the chattering, but has no steady state error and keeps the system on the sliding line S=0.

b) The ideal saturation control.

The switching law, shown in Figure 3.2, is given by

$$u(s) = sat(s) = \begin{cases} +1 \ , & s(x) > L \\ \dfrac{s}{L} \ , & |s(x)| \le L \\ -1 \ , & s(x) < -L \end{cases} \tag{3.11}$$

where $\mp L$ represents threshold of entering the boundary layer.

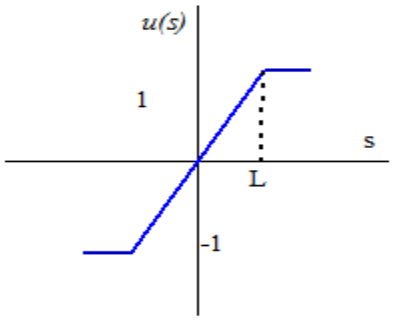

Figure 3.2: The ideal saturation relay.

The control inside the limits $\mp L$ has high gain property, while outside it has ideal relay behavior. The combination of both control laws vanishes the sliding mode because the trajectories are not forced to stay on $s = 0$. If there is no disturbance there will be no steady error, and no chattering also.

c) The practical ideal relay

Figure 3.3 shows its construction. The control input is given by

$$u(s) = hys(s) = \begin{cases} +1 \ , \ where \ s(x) > \Delta \\ -1 \ , \ where \ s(x) < \Delta \end{cases} \tag{3.12}$$

where $2\Delta > 0$ represents the hysteresis band in *s(x)*. The relay has the hysteresis nature, which makes it impossible to switch on the sliding line *s=0*; instead it will switch such that $s = \pm\Delta$.

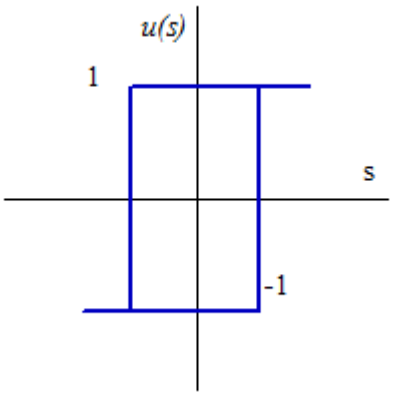

Figure 3.3: Practical ideal relay.

This control input produces non-ideal sliding mode which always includes chattering for the state and eliminating chattering problem becomes impossible.

d) The practical saturation control

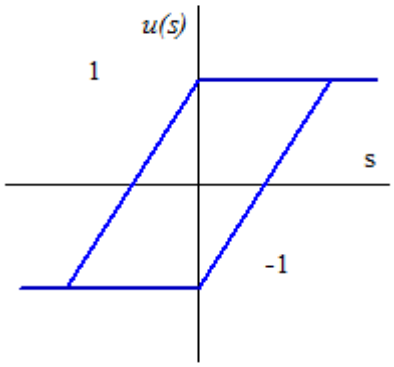

Figure 3.4: Practical saturation relay.

This is shown in Figure 3.4 and it's close to the practical relay control but has saturation behavior which makes it difficult to analyze for linear and nonlinear systems. Using this control input eliminates the sliding mode completely. The system is asymptotically stable in the large, but has two equilibrium points.

3.4 Three-level Hysteresis Function

In [9] the authors propose a three-level hysteresis function derived from the voltage error. The voltage error (x1) and its derivative (x2) are multiplied by k_1 and k_2, respectively. The resulting switching function is applied to a three-level comparator. The sliding surface is defined as

$$s(x) = k_1 x_1 + k_2 x_2 \tag{3.13}$$

The amplitude of the hysteresis band is chosen such that the switching frequency for the three level function is 3.5KHz. Figure 3.5 shows the main construction of the controller proposed there. The values of k_1 and k_2 are not given in the paper and derived from optimization of a function.

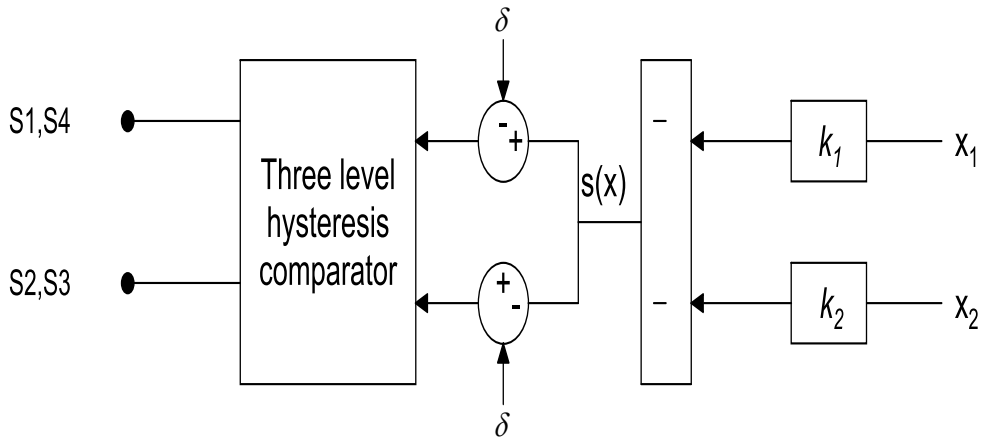

Figure 3.5: Main feature of the controller proposed in [9].

The parameter δ represents the amplitude of the hysteresis band and is introduced in order to limit the switching frequency. The disturbance equation is obtained in direct relationship with the load current as

$$d = -\frac{1}{C}\left(\frac{di_L}{dt}\right) - \frac{R}{LC} i_L \tag{3.14}$$

The simulation shows that the controller is very slow and unable to track the reference signal. Big undershoot and overshoot are noticed. The dynamics of the controller are unsatisfactory due to the load variation. This problem has been eliminated in the next approach by suitably choosing the hysteresis width and by applying the integral term to the voltage error.

3.5 An Improved Three-level Hysteresis Function

A three level hysteresis function is also applied in [5], where the theory of sliding mode control is applied to the inverter system. Referring to Figure 3.6 the system equations could be derived as follows.

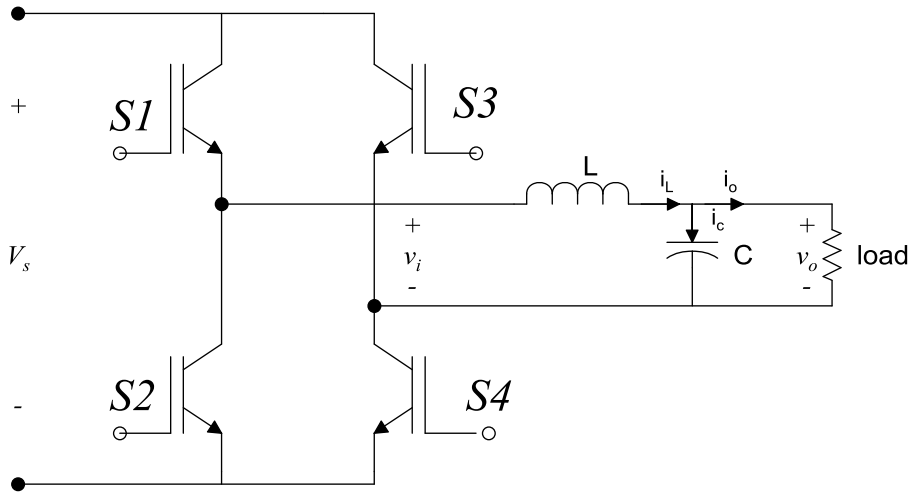

Figure 3.6: UPS inverter system.

The inductor current and voltage are given by

$$L\frac{di_L}{dt} = v_i - v_o \tag{3.15}$$

$$i_L = i_C + i_o \tag{3.16}$$

Where v_i is the filter input voltage, and v_o is the output voltage. The inductor current, the capacitor current and the output current are i_L, i_C and i_o as shown in the figure. The voltage error and its derivative are defined as

$$x_1 = v_o - v_{o,ref} \tag{3.17}$$

$$x_2 = x_1^{\bullet} = v_o^{\bullet} - v_{o,ref}^{\bullet} \tag{3.18}$$

where $v_{o,ref} = V_m \sin(wt)$ is the sinusoidal reference voltage.

The sliding function is established from the voltage error, the voltage error rate of change and its integral as

$$s(x) = \alpha x_1 + x_2 + \beta x_3 \tag{3.19}$$

where s(x) is the sliding surface, x_1 is the voltage error, x_2 and x_3 are the rate of change and the integral of the voltage error. Figure 3.7 shows the main structure of the sliding mode controller.

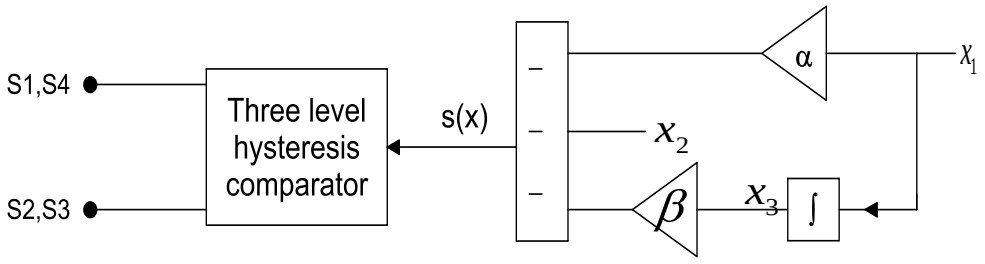

Figure 3.7: Main features of the three level hysteresis controller [5].

The sliding function enters a three-level comparator. When the switching function value reaches the upper level of the comparator, the inverter switches switch such that a negative voltage is applied to the inverter output (to the filter input), and when

the switching function reaches the lower hysteresis level, the inverter switches switch such that a positive voltage is applied.

The comparator nature implies that the switching frequency will vary in a wide range. One of the main design issues when this controller is used, is to design and adjust the value of the hysteresis band; this value reduces the chattering problem, which could be defined as the zigzag behavior of the state around, $s(x) = 0$ which occurs when the state asymptotically approaches the equilibrium point.

Authors of [5] have derived an equation for the estimated switching frequency of the system when three-level and two-level hysteresis comparators are used. The derived equations have been confirmed through simulation and experimental results. The estimated average switching frequency for three-level hysteresis switching function is seen to be much lower than two-level hysteresis.

An equation of the hysteresis boundary is derived in direct relationship with the system parameters. The equation specifies the minimum and the maximum possible values of the output current rate of change and helps directly to define the limits of the hysteresis band which will be applied to the controller.

The proposed approach shows a very good disturbance rejection at low harmonic distortion when nonlinear and sudden load are applied, while this was not possible using the three-level function proposed in [9]. This is because of the suitable choice and implementation of the hysteresis boundary and because of the integral term was added to the sliding function term.

3.6 Rotating Sliding Mode

In [6], the sliding line rotates in the phase plane such that the output voltage follows its reference. The slope of the sliding line is derived from input/output relationships of fuzzy logic rule [8]. The slope of the sliding line is defined

$$\lambda^{FL}(t) = -0.45X_d(t) + 0.5 \tag{3.20}$$

where $|x_1|$, $|x_2|$ are the instantaneous absolute value of the voltage error and its derivative, respectively. $X_d(t)$ is defined as $|X_d(t)| = |x_1| - |x_2|$. The sliding surface is defined as

$$s(x) = \lambda^{FL}(t)x_1 + x_2 \tag{3.20}$$

Figure 3.8 shows the main concept of the proposed controller

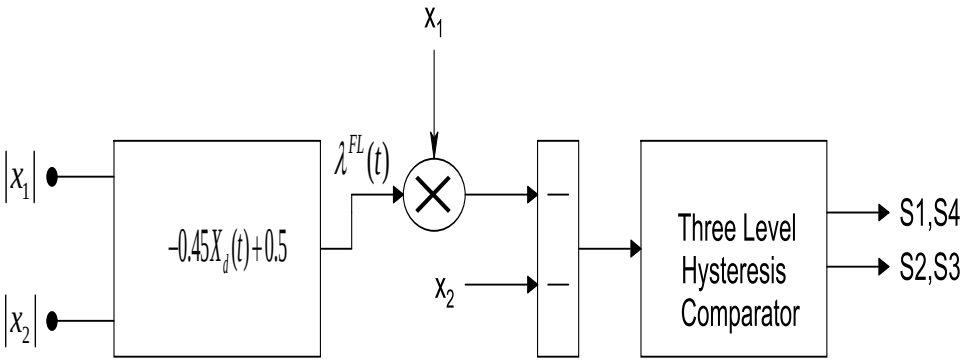

Figure 3.8: Main features of the RSMC controller [6].

As shown before in [5], reducing steady state error is possible if the hysteresis width is reduced. But the problem of the chattering will arise when load variation is applied to the load side. This directly affects the robustness of the system. This is the first problem to be solved here. The second problem is to reduce the reaching time for the error state at load variation.

The author of [5] has proposed a function for the sliding line slope which is continuously computed such that the tracking performance of the inverter is improved. Simulation of the proposed method shows that the controller is capable of solving the previous two problems when disturbance occurs.

Chapter 4

SMC APPLIED TO UPS INVERTER

In this part, the theory of sliding mode control is going to be applied to the UPS system. Problem formulation and control function derivation are presented. Saturated control function is applied using feedback control to the inverter switches.

A discussion about the possible mistakes that the authors of [7] have fallen in will be presented. Arguments will be presented, showing the considerations to be taken such that the proposed function works properly.

4.1 Mathematical Formulation

Figure 4.1 shows a single phase UPS inverter.

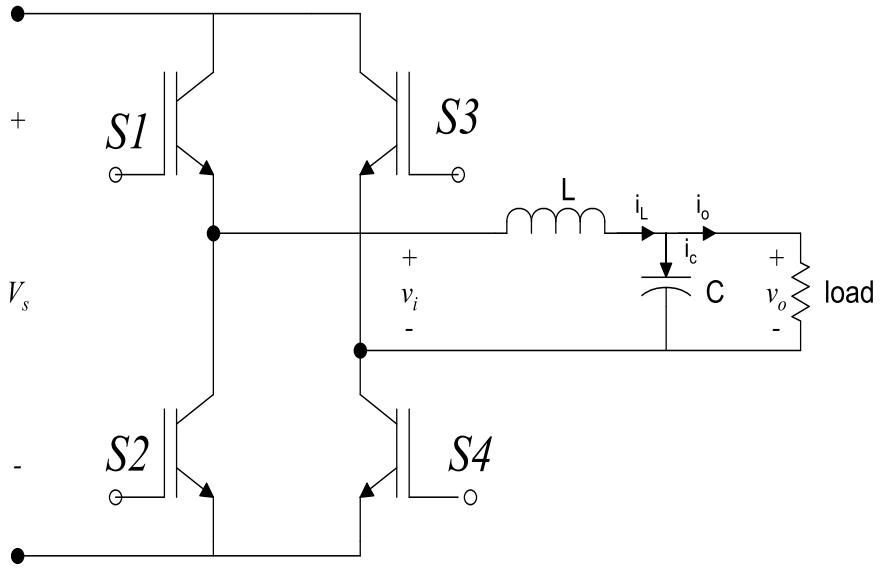

Figure 4.1: UPS inverter.

The LC filter equations are

$$L\frac{di_L}{dt} = v_i - v_o \tag{4.1}$$

$$i_L = i_c + i_o \tag{4.2}$$

The term v_i is defined to be the inverter output voltage before the filter, which is produced by multiplication of the control input by the DC source voltage $v_i = uV_s$. The voltage error and the error rate are defined as

$$x_1 = v_o - v_{o,ref} \tag{4.3}$$

$$x_2 = x_1 = v_o^{\bullet} - v_{o,ref}^{\bullet} \tag{4.4}$$

where v_{ref} is the reference voltage $v_{ref} = V_m \sin(wt)$. The above equations represent the system equations which can be written as [5]

$$x_1^{\bullet} = x_2 \tag{4.5}$$

$$x_2^{\bullet} = \omega_o^2[-x_1 + uV_s + DV_s] \tag{4.6}$$

where D is the disturbance term given by

$$D = \frac{-L}{V_s}\frac{di_o}{dt} - \frac{v_{ref}}{V_s} - \frac{LC}{V_s}\frac{dv_{ref}^{\bullet}}{dt} \tag{4.7}$$

A suitable switching condition should be established to ensure that all the states will reach the sliding surface. The condition is given by [7]

$$\lambda(\lambda - \frac{1}{RC}) > -\frac{1}{LC} \tag{4.8}$$

After designing the switching condition, the sliding surface is defined as

$$s(x) = \lambda x_1 + x_2$$

which is simplified to be

$$s(x) = (\lambda - \frac{1}{RC})\Delta v_O + \frac{1}{c}\Delta i_L \tag{4.9}$$

The details are provided in appendix A.

4.2 Switching Controller

After designing the sliding surface, the switching control function is to be designed. This thesis provides correction for the proposed controller in [7] (the argument points will be discussed later). Here, a saturation control function is to be used. Figure 4.2 shows the main construction of the proposed controller characteristic.

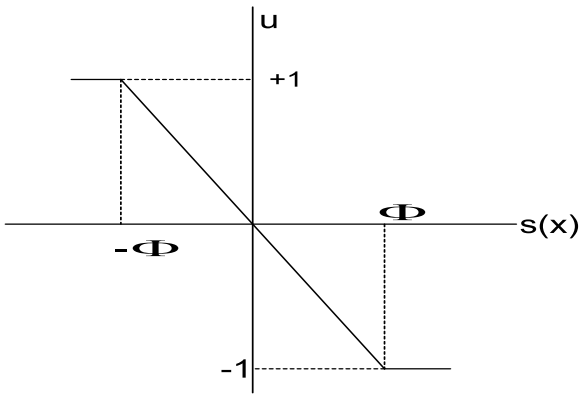

Figure 4.2: Saturation control function (smooth control law).

The proposed smooth control law is designed to eliminate or reduce the problem of chattering as discussed before in section 3.4. The smoothed control output is compared with a carrier wave using a two-level PWM comparator, as shown in Figure 4.3.

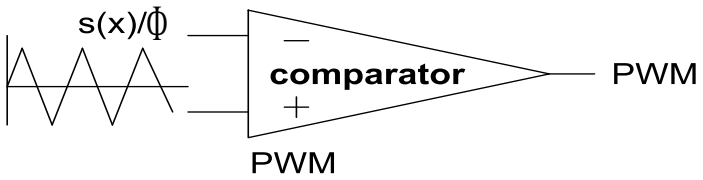

Figure 4.3: Two level PWM comparator.

The output voltage will be unipolar as discussed in Section 2.3. The comparator will work properly if the slope of $\frac{s(x)}{\Phi}$ is smaller than the slope of the carrier wave. Referring to Figure 4.4, the magnitude of the carrier slope is given by

$$\left|slope_{carrier}\right| = \frac{2V_p}{\frac{1}{2}T_s} = 4V_p f_s \tag{4.10}$$

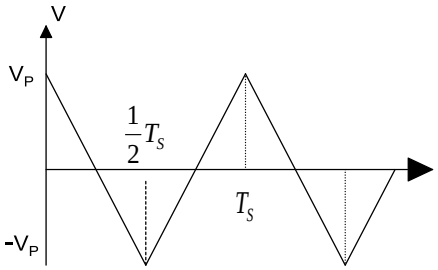

Figure 4.4: Carrier signal.

The current ripple is given by $\Delta i_L = \frac{\left|\Delta i_L\right|}{d.T_s} = \frac{V_s}{L}(1-\left|u\right|)$ and the sliding surface is given by

$$s(x) = \left(\lambda - \frac{1}{RC}\right)\Delta v_o + \frac{1}{c}\left|\Delta i_L\right| \tag{4.11}$$

Assuming that $\left(\lambda - \frac{1}{RC}\right)\Delta v_o << \frac{1}{C}\Delta i_L$, which means that the ripple current value is much greater than the sliding line slope multiplied by the voltage error. Then $s(x)$ is given by $s(x) = \frac{1}{c}\Delta i_L$ and

$$\frac{s(x)}{\Phi} = \frac{1}{C\Phi}\Delta i_L \tag{4.12}$$

Now the maximum possible value of the current ripple occurs when the control input $\left|u\right| = 0$. The lower bound for the parameter Φ becomes

$$\Phi >> \frac{V_s}{4V_p LCf_s} \tag{4.13}$$

This value represents the minimum value of the saturation layer boundary. This is the second wrong assumption corrected in [7]; further discussion will be given in the next section.

4.3 Arguments

The proposed control method in [7] has failed to derive a true switching function to control the system; there are mistakes in the assumption, calculation and in the simulation. Here modifications to their approach are presented. Arguments are as follows.

4.3.1 Failure in the Inductor Current Ripple Assumption

The authors of [7] have assumed that the ripple in the inductor current is equal to the capacitor current ripple, which is not true. Here is the mathematical derivation. The inductor current and output voltage are (shown in Figure 4.5)

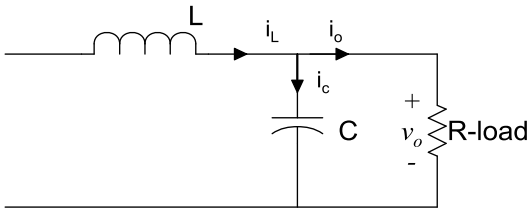

Figure 4.5: UPS filter output.

$$i_L = i_c + i_o \tag{4.14}$$

$$\Delta v_o = v_o - v_{ref} \tag{4.15}$$

From (4.15) the output voltage is

$$v_o = \Delta v_o + v_{ref} \tag{4.16}$$

and the capacitor current ripple is

$$i_c - i_{ref} = i_L - i_o - i_{c,ref} = \Delta i_c \tag{4.17}$$

Substitute (4.17) in

$$\Delta i_c = \Delta i_L - \frac{v_o}{R} - C\frac{dv_{ref}}{dt} = i_L - \frac{\Delta v_o}{R} - \left(\frac{v_{ref}}{R} + C\frac{dv_{ref}}{dt}\right) \tag{4.18}$$

the final equation for capacitor current ripple is

$$\Delta i_c = \Delta i_L - \frac{\Delta v_o}{R} \tag{4.19}$$

So the capacitor current ripple is less than the inductor current ripple by $\frac{\Delta v_o}{R}$.

4.3.2 Choosing Minimum Value of Saturation

The authors of [7] have chosen the value of Φ as

$$\Phi >> \frac{V_S}{16LCf_sV_p} \tag{4.20}$$

This assumption is not true. For the given carrier signal, the lower bound of Φ is to be calculated as shown in the previous section 4.2 to be

$$\Phi >> \frac{V_S}{4LCf_sV_p} \tag{4.21}$$

4.3.3 Contradiction with the Given Value of Φ When Parameters Are Substituted

There is contradiction between the given value of Φ and the calculated value when the given system parameters are substituted in the equations. There are two probabilities: either the given filter parameters are not true or the given minimum saturation value is not true.

Even though if we assume that the given equation of Φ is true, still the simulated value given in the published work is much lower than the calculated one from the given parameters. If it would be calculated from the given filter parameters, carrier peak voltage and the given switching frequency, the minimum value of Φ to be used in the hysteresis band (h) is Φ=543213. Instead they have used a lower value (Φ =134751). This part is not understandable in [7].

4.3.4 Calculation of the Control Input

To assure that our assumption is true, the control input has been calculated. It should be less than one. The detailed calculations are given in Appendix B. The control input amplitude is obtained as

$$U_m = \left|U(j\omega)\right| = \left[\frac{\lambda^2 + \omega^2}{(\phi + \lambda a - \omega b)^2 + (\omega a + \lambda b)^2}\right]^{1/2} V_m \tag{4.21}$$

where λ is the sliding line slope, $a = V_s A\cos\alpha$ and $b = V_s A\sin\alpha$. The constant *A* is given by

$$A = \frac{1}{\sqrt{\left(1-\omega^2 LC\right)^2 + \omega^2\left(\frac{L}{R}\right)^2}} \tag{4.22}$$

and the angle α is defined by $\alpha = -\tan^{-1}\left(\frac{\omega L}{R(1-\omega^2 LC)}\right)$.

The following table concludes the previous discussion and shows the value of the control input and the value of error from the derived mathematical equations and when Matlab/Simulink toolbox is used.

Table 4.1: Calculated and simulated value of ϕ for the given new system parameters.

$\Phi\ (V/s)$	Calculation		Simulation	
	U_m	Δv_o (volt)	U_m	Δv_o (volt)
60000	0.873	3.49	0.942	3.72
150000	0.859	8.59	0.908	9.02
250000	0.843	14.05	0.89	14.62

The calculated and the simulated values of Φ given in Table 4.1 correspond to the parameters given in Table 4.2. A new PWM is derived with carrier peak voltage equal to one.

Table 4.2: System and controller parameters

L	1 mH
C	100 μF
f_s	15KHz
$\Phi_{\min}$	58333 V/S
V_{ref}	220 Volt (rms)
V_S	350 Volt
S_{out}	6 KVA
R	9.54 Ω
λ	15000
Carrier Amplitude	1 Volt

Figure 4.8 shows the relationship between the control input and the saturation parameter. Figure 4.6 is plotted from equation (4.21) and using the parameters given in Table 4.2. As expected, the control input (U) increases when saturation value is decreased, which is clear from the equation.

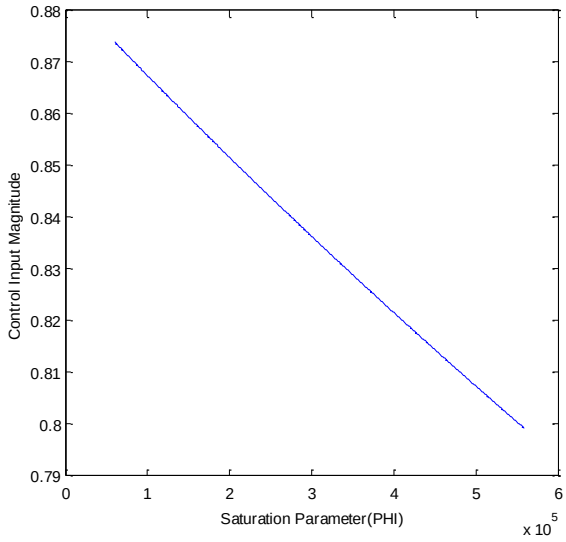

Figure 4.6: Control input magnitude in relation with saturation parameter.

The voltage error increases with the increase of the saturation parameter as shown in Figure 4.7.

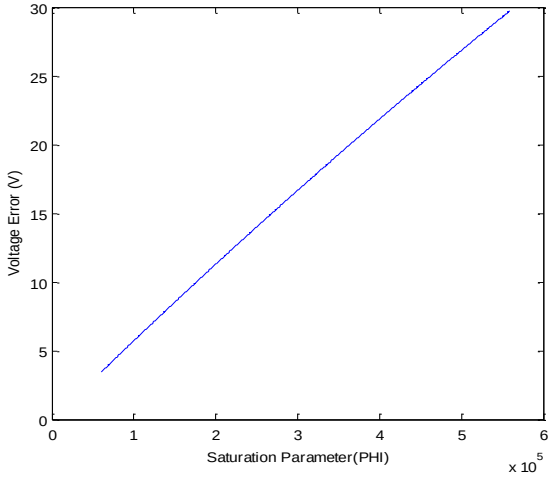

Figure 4.7: Output voltage error in relation with saturation parameter.

Chapter 5

COMPUTER SIMULATIONS

5.1 Introduction

In this chapter the SMC theory using the saturation function is to be applied to the UPS inverter. Matlab/Simulink toolbox is used for simulation. The proposed approach is investigated under different conditions to ensure its validity. A resistive load ($R = 9.54\Omega$) is applied to the inverter load side, which represents the linear load. The same resistive value is suddenly applied to the system, so the controller behavior can be investigated under transient conditions.

A full-bridge rectifier load is used to simulate the case when a nonlinear load is applied. The nonlinear load used here is according to IEC62040-3 standard, which requires that the total harmonic distortion (THD) value is to be less than 5% for the output voltage. Full-bridge rectifier used here has input resistance $R_s = 0.32\Omega$, and with parallel RC circuit $R = 18\Omega$ and $C = 8200\mu F$.

The proposed method was simulated for saturation function value $\Phi = 60000$. This value had been chosen to be greater than the specified threshold. The inverter parameters are given in Table 4.2.

5.2 Fixed Switching Frequency SMC with Linear Load

Figure 5.1 shows the simulink model for fixed switching frequency SMC when linear load is applied, the contents of the subsystem shown in Figure 5.1 are given in appendix C which represents the switching block.

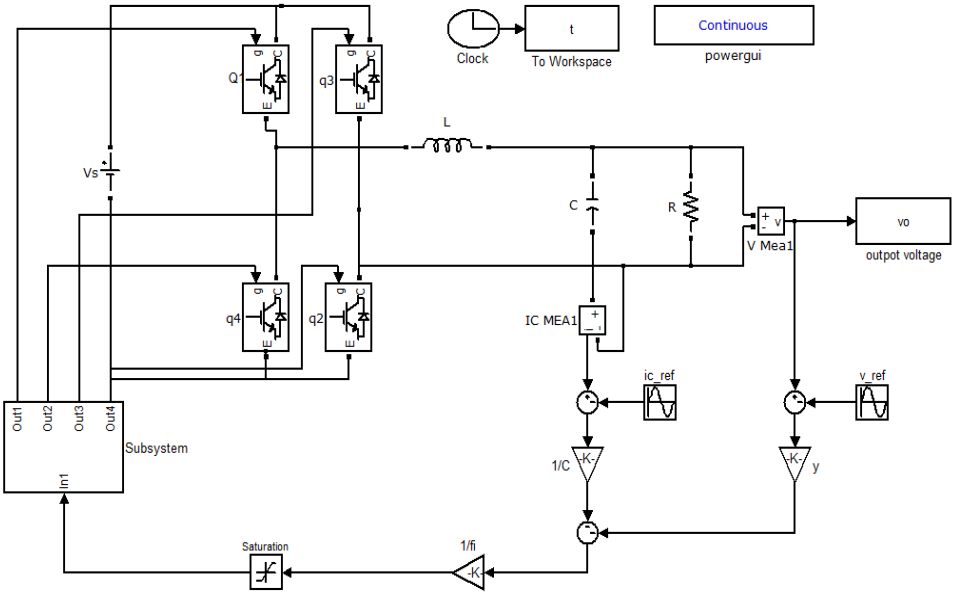

Figure 5.1: Simulink model for fixed switching frequency SMC with linear load.

The voltage and current output waveforms are shown in Figure 5. 2.

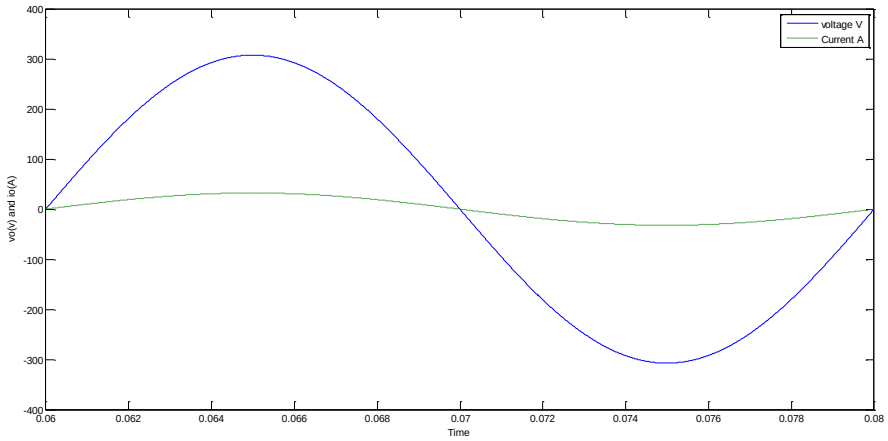

Figure 5.2: Output voltage and current waveforms for linear load at ϕ =60000.

When linear load is applied, the peak error voltage was measured to be 3.72 volt. Figure 5.3 shows the measured output voltage error, while the current rate of change reaches to 1.5×10^4 A/s as shown in Figure 5.4.

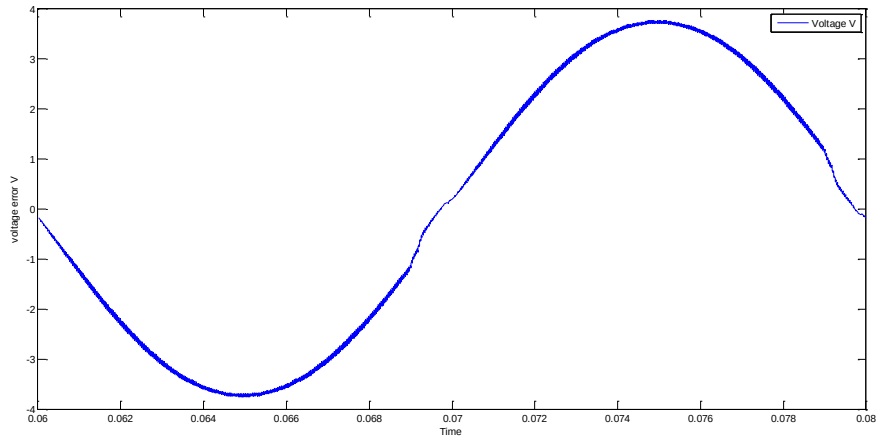

Figure 5.3 Output voltage error waveform for linear load at ϕ =60000.

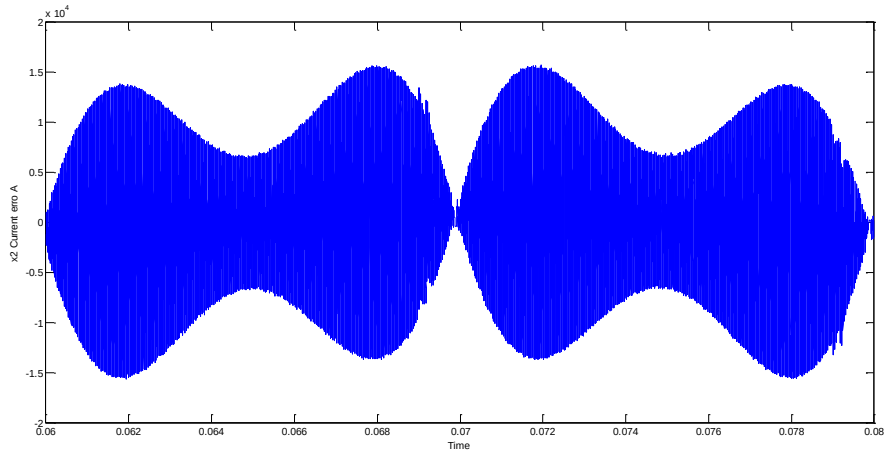

Figure 5.4 Current rate of change error waveform for linear load at ϕ =60000.

5.3 Fixed Switching Frequency SMC with Sudden Load

A sudden load is applied to the inverter as shown on Figure 5.5. The peak of the output voltage reaches to 307.4 volt when $\Phi = 60000$. The voltage and current output waveforms are shown in Figure 5. 6 and Figure 5.7.

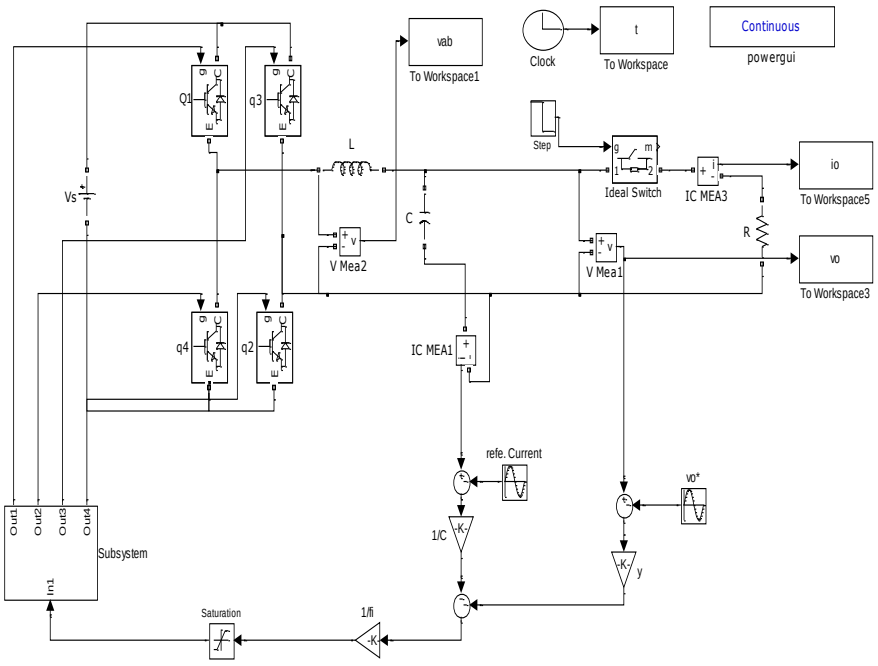

Figure 5.5: Simulink model for fixed switching frequency SMC for sudden load [5].

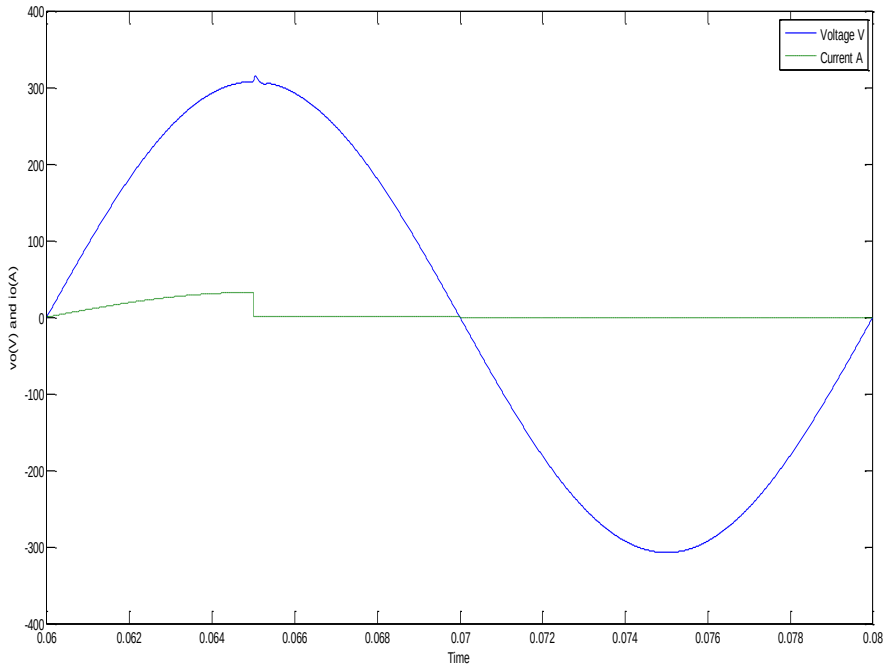

Figure 5.6 Output voltage and current waveforms for sudden load at ϕ =60000.

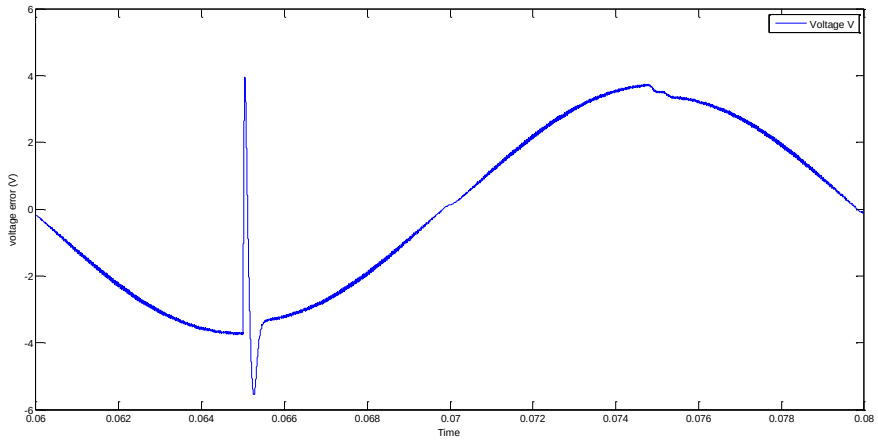

Figure 5.7 Output voltage error waveforms for sudden load at ϕ =60000.

Overshoot and undershoot were observed when sudden load is applied with values of 3.5×10^{5} and -0.5×10^{5}, respectively. The controller was able to handle the disturbance, and a good tracking capability is noticed. Disturbance rejection and the robustness of the controller are satisfactory as shown in Figure 5.8.

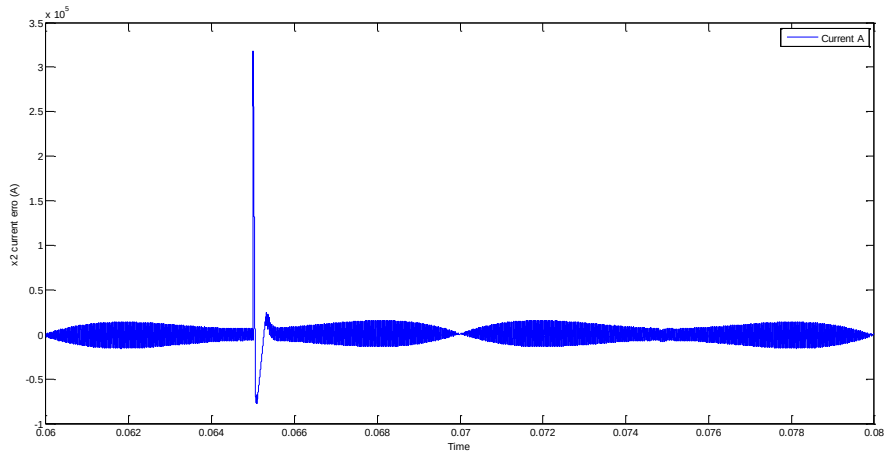

Figure 5.8: Current error waveform for sudden load at ϕ =60000.

5.4 Fixed Switching Frequency SMC with Nonlinear Load

Figure 5.9 shows the Simulink model for fixed switching frequency SMC when nonlinear load is applied. The voltage and current output waveforms are shown in Figure 5.10.

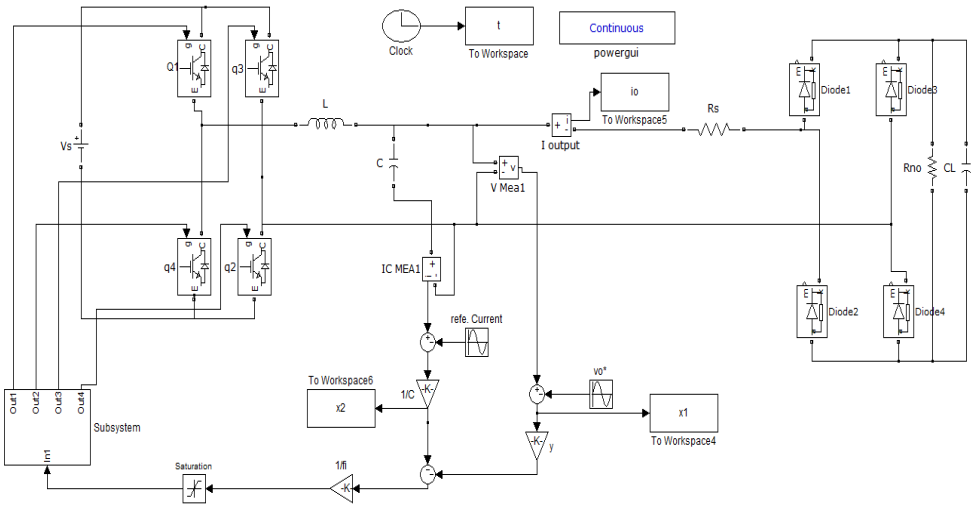

Figure 5.9: Simulink model for fixed switching frequency SMC with nonlinear load.

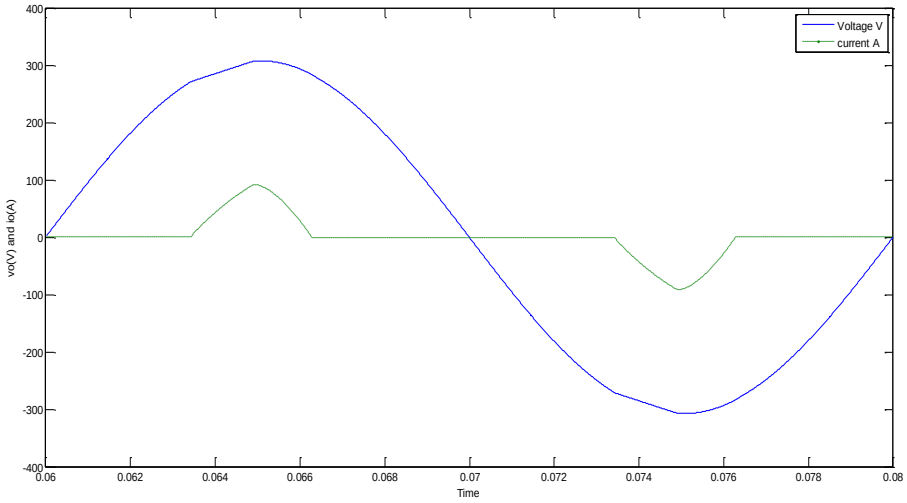

Figure 5.10: Output voltage and current waveforms for nonlinear load at $\phi = 60000.$

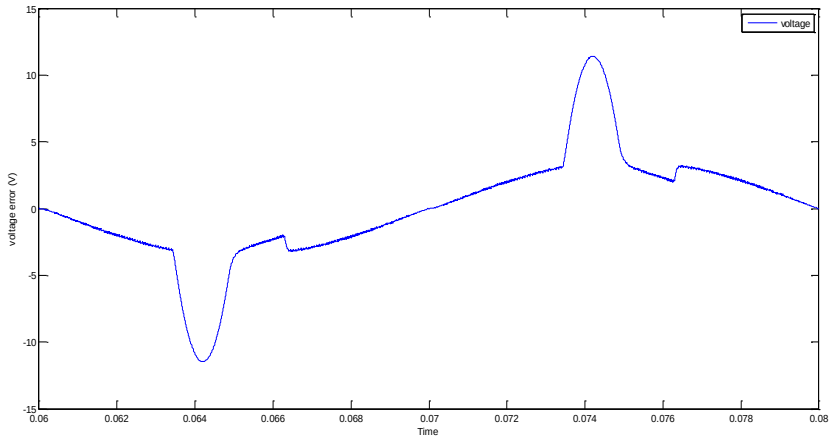

Figure 5.11: Output voltage error waveforms for nonlinear load at ϕ =60000.

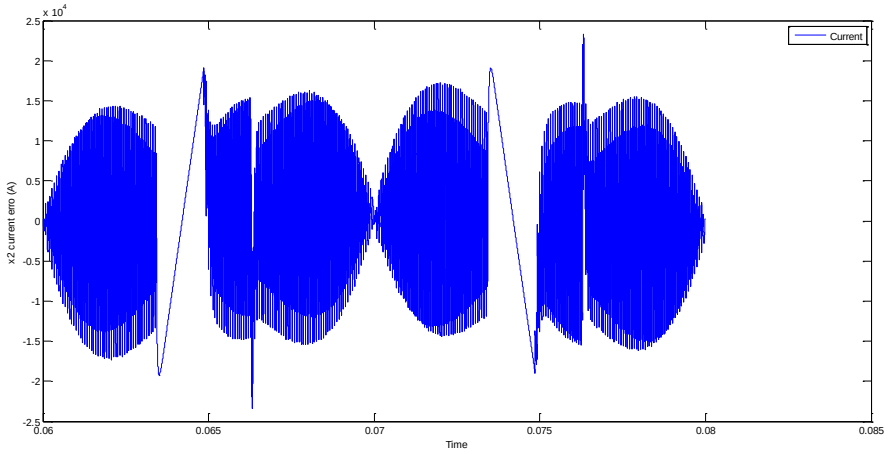

Figure 5.12: Current error waveform for nonlinear load at ϕ =60000.

Table 5.1 summarizes the above results for all load types. The controller shows a proper response to parameter variations with low total harmonic distortion according to IEC62040-3 [7].

Table 5.1: Output results for different loads at ϕ =60000.

	R_Load	Nonlinear load	Sudden Load
Output Voltage(V)	307.4	307.8	307.4
Error(V)	3.72	3.32	3.72
THD(%)	0.0404	1.14	0.0381

5.5 Resonance Compensator

Figure 5.15 shows the Simulink model for fix switching frequency SMC when linear load is applied with resonant compensator

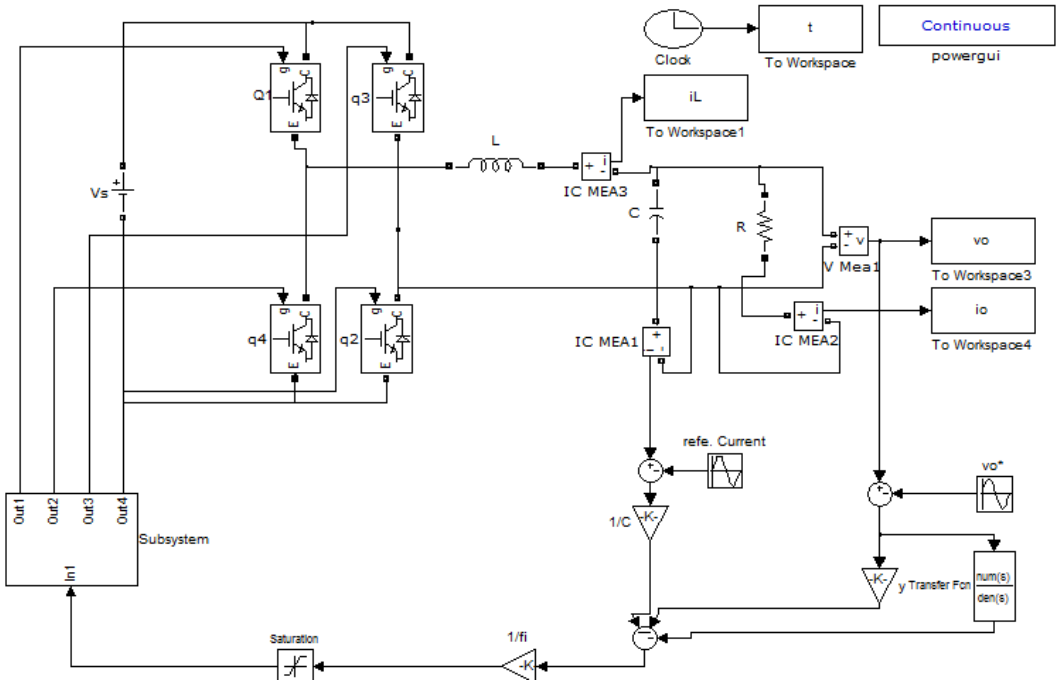

Figure 5.13: Simulink model of SMC for linear load with resonant compensator.

The voltage and current output wave form are shown in figure 5.14.

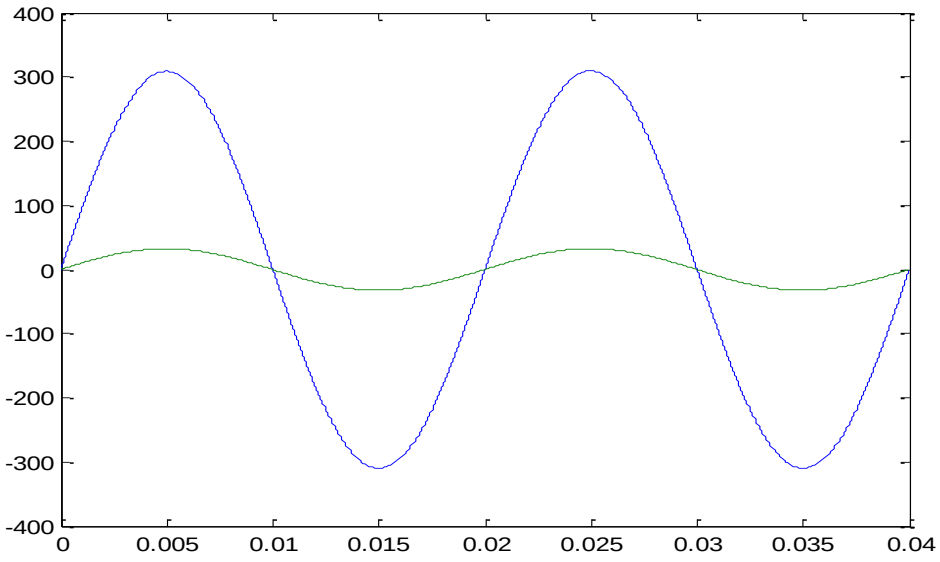

Figure 5.14: Output voltage and current waveforms for linear load with resonant compensator at ϕ=60000.

In order to improve the effectiveness of the proposed controller, resonance compensator was installed in the feedback loop of the control input to compensate for the voltage error. We note the output voltage is improved and the voltage error decreased.

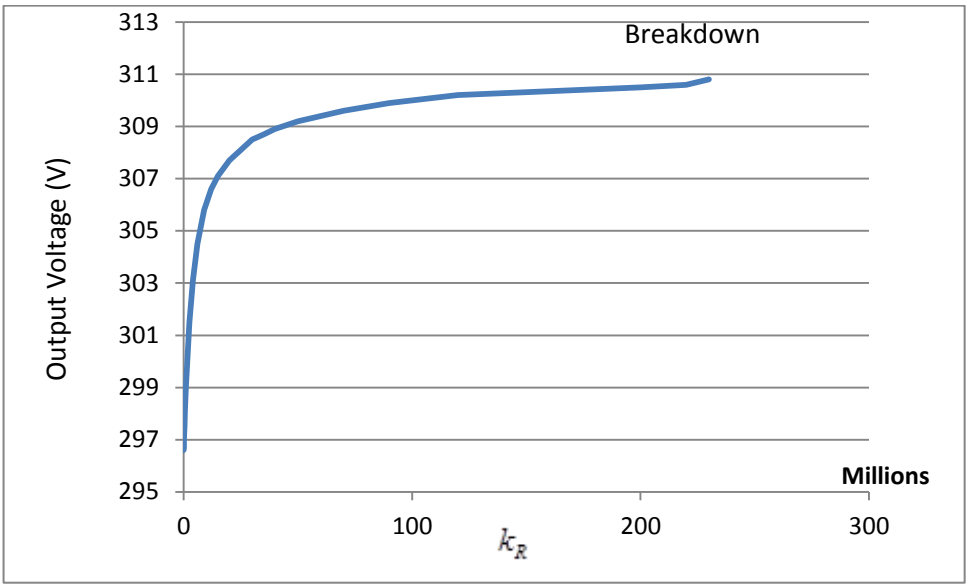

Figure 5.15: Relationship between k_R and output voltage waveform.

The ideal resonance compensator equation is given by

$$G(s) = k_p + \frac{k_R s}{s^2 + w_R^2} \tag{5.1}$$

For a practical resonance compensator, the value of the proportional term k_p is equal to zero. The practical compensator given in (5.2) has damping resonance frequency $w_R = 2\pi 50\,\text{rad/s}$.

$$G(s) = k_p + \frac{k_R s}{s^2 + w_R s + w_R^2} \tag{5.2}$$

For different values of the constant k_R, the compensator was tested. Figure 5.13 shows the relationship between the compensator increment and the amplitude of the output voltage till it reaches the breakdown stage.

Chapter 6

CONCLUSION AND FUTURE WORK

6.1 Conclusion

The theory of sliding mode control is applied to the UPS inverter. The proposed controller has been derived on the basis of linearity of the controller output in a narrow layer such that the problem of chattering is reduced. PWM is used to compare a carrier signal with the smoothed control function, resulting in fixed switching frequency of the unipolar inverter. The proposed control method has been derived and confirmed on a mathematical basis.

Simulation using matlab/Simulink toolbox of the proposed controller under linear, nonlinear and sudden loads shows the effectiveness of the controller. Low total harmonic distortion of the output voltage was observed. The controller has fast tracking of the reference signal and good disturbance rejection to load variations.

6.2 Future Work

As an extension to the work proposed here, a practical implementation to the proposed method may be done. Application to three-phase UPS inverters may be considered. The proposed controller could be applied for the utilization of renewable energy, such as grid-connected inverter applications. Furthermore, it could be applied for improving the power factor.

REFERENCES

[1] B. M. Wilamowski & J. D. Irwin, *The Industrial Electronics Handbook Power Electronic and Motor Drives*, 2nd ed., CRC Press: Taylor & Francis, 2011.

[2] B. K. Bose, *Modern Power Electronics and AC Drives*, Prentice Hall, Upper Saddle River, 2002.

[3] M. H. Rashid, *Power Electronics Handbook*, Academic Press, 2001.

[4] Bose, & Bimal K. "Recentadvances in power electronics," *IEEE Transactions on Industrial Electronics*, vol. 7, no. 1, pp. 2-16, 1992.

[5] O. Kukrer, H. Komurcugil, & A. Doganalp, "A three-level hysteresis function approach to the sliding-mode control of single-phase UPS inverters," *IEEE Transactions on Industrial Electronics*, vol. 56, no. 9, pp. 3477-3486, 2009.

[6] H. Komurcugil, "Rotating-sliding-line-based sliding-mode control for single-phase UPS inverters." *IEEE Transactions on Industrial Electronics*,vol. 59, no. 10, pp. 3719-3726, 2012.

[7] A. Abrishamifar, A. Ahmad, & M. Mohamadian, "Fixed switching frequency sliding mode control for single-phase unipolar inverters," *IEEE Transactions on Power Electronics*, vol. 27, no. 5, pp. 2507-2517, 2012.

[8] F. Yorgancioglu & H. Komurcugil, “Single-input fuzzy-like moving sliding surface approach to the sliding mode control,” *Electrical Engineering*, vol. 90, no. 3, pp. 199-207, 2008.

[9] Carpita, M., P. Farina, & S. Tenconi, "A single phase, Sliding Mode Controlled Inverter with three levels output voltage for UPS or Power Conditioning Applications," pp. 272-277, 1993.

[10] Gao, Weibing, & James C. Hung, "Variable structure control of nonlinear systems: a new approach," *Fifth European Conference In Power Electronics and Applications*, vol. 40, no. 1, pp. 45-55, May 1993.

[11] Hung H. J., W. Gao, & C. J. Hung, "Variable structure control: a survey," *IEEE Trans. on Industrial Electronics*, vol. 40, no. 1, pp. 2-22, February 1993.

[12] Timothy L. Skvarenina, *The Power Electronics Handbook Industrial Electronics Series*, 2nd ed. CRC Press, 2002.

APPENDICES

Appendix A: Derivation of Equation (4.9)

From the theory of sliding mode we know that

$$s(x) = \lambda x_1 + x_2 = \lambda \Delta v_o + \frac{1}{C}\left(i_c - i_{c,ref}\right) \tag{A.1}$$

The voltage error is defined as $\Delta v_o = v_o - v_{ref}$. If the inductor current is given by $i_L = i_c + i_o$, then the capacitor current error is given by

$$i_c - i_{c,ref} = (i_L - i_o) - i_{c,ref} = \Delta i_c \tag{A.2}$$

Substituting the output current and the capacitor current we have

$$\Delta i_C = i_L - \frac{v_o}{R} - C\frac{dv_{ref}}{dt} = i_L - \frac{\Delta v_o}{R} - \left(\frac{v_{ref}}{R} + C\frac{dv_{ref}}{dt}\right) \tag{A.3}$$

Such that $i_{L,ref} = \frac{v_{ref}}{R} + C\frac{dv_{ref}}{dt}$. Simplify the terms $\Delta i_C = \Delta i_L - \frac{\Delta v_o}{R}$, the sliding surface is obtained as

$$s(x) = \lambda \Delta v_o - \frac{1}{RC}\Delta v_o + \frac{1}{C}\Delta i_L \tag{A.4}$$

$$s(x) = \left(\lambda - \frac{1}{RC}\right)\Delta v_o + \frac{1}{C}\Delta i_L \tag{A.5}$$

Appendix B: Derivation of Equation (4.21)

Let the control input is defined by $u = U_m \cos(\omega t + \phi_m)$ and the reference voltage is $v_{ref} = V_m \cos \omega t$. The transfer function of the filter output is given by

$$H(s) = \frac{v_o(s)}{v_{inv}(s)} = \frac{R}{R + sL + s^2 RLC} \tag{B.1}$$

which becomes $H(j\omega) = \dfrac{1}{(1-\omega^2 LC) + j(\omega \dfrac{L}{C})}$ in the frequency domain. When the control input is applied to (B.1), the output voltage is

$$v_o(j\omega) = V_s U_m \left| H(j\omega) \right| e^{j(\phi_m + \varphi(j\omega))} \tag{B.2}$$

The magnitude defined to be A is given by

$$A = \left| H(j\omega) \right| = \frac{1}{\sqrt{(1-\omega^2 LC)^2 + \left(\omega \dfrac{L}{R}\right)^2}} \tag{B.3}$$

And angle $\alpha = \varphi(j\omega) = -\tan^{-1}\left(\dfrac{\omega L}{R(1-\omega^2 LC)}\right)$.

Then the voltage is $v_o(t) = V_s U_m \left| H(j\omega) \right| \cos\left(\omega t + \phi_m + \varphi(j\omega)\right)$ and the voltage error is given by

$$\Delta v_o = v_o - v_{ref} = V_s U_m \left| H(j\omega) \right| \cos\left(\omega t + \phi_m + \varphi(j\omega)\right) - V_m \cos \omega t \tag{B.4}$$

The sliding surface is given by

$$\sigma(x) = \frac{s(x)}{\Phi} = \frac{\lambda}{\Phi} \Delta v_o + \frac{1}{\Phi} \frac{d}{dt} \Delta v_o \tag{B.5}$$

And the control input is the negative of (B.5)

$$u = -\sigma = -\frac{\lambda}{\Phi} \Delta v_o - \frac{1}{\Phi} \frac{d}{dt} \Delta v_o \tag{B.6}$$

At steady state, the control input magnitude is

$$U(j\omega) = -\frac{1}{\Phi}(\lambda + j\omega)\left(v_o(j\omega) - v_{ref}(j\omega)\right) \tag{B.7}$$

For simplicity; defining a constant $\gamma = \frac{\lambda + j\omega}{\Phi}$ .Then $U(j\omega) = -\gamma\left[V_s u(j\omega)H(j\omega) - V_m\right]$ which could be written as

$$U(j\omega) = \frac{\gamma V_m}{1 + \gamma V_s H(j\omega)} = \frac{(\lambda + j\omega)V_m}{\Phi + (\lambda + j\omega)V_s A(\cos\alpha + j\sin\alpha)} \tag{B.8}$$

Define

$$a = V_s A\cos\alpha \tag{B.9}$$

$$b = V_s A\sin\alpha \tag{B.10}$$

The control input is further simplified as

$$U(j\omega) = \frac{(\lambda + j\omega)V_m}{(\Phi + \lambda a - \omega b) + j(\omega a + \lambda b)} \tag{B.11}$$

From (B.11), the magnitude of the control input is given by

$$U_m = |U(j\omega)| = \left[\frac{\lambda^2 + \omega^2}{(\Phi + \lambda a - \omega b)^2 + (\omega a + \lambda b)^2}\right]^{\frac{1}{2}} V_m \tag{B.12}$$

And the voltage error magnitude is

$$|\Delta v_o(j\omega)| = \frac{\Phi U_m}{\sqrt{\lambda^2 + \omega^2}} = \frac{\Phi V_m}{\sqrt{(\Phi + \lambda a - \omega b)^2 + (\omega a + \lambda b)^2}} \tag{B.13}$$

Appendix C: Switching block content: